One-Bond ($^{1d}J_{H-H}$) and Three-Bond ($^{3d}J_{X-M}$) Spin−Spin Coupling Constants Across X−H···H−M Dihydrogen Bonds

Janet E. Del Bene,*,†,‡ S. Ajith Perera,† Rodney J. Bartlett,† Ibon Alkorta,§ José Elguero,§ Otilia Mó,|| and Manuel Yáñez||

Quantum Theory Project, University of Florida, Gainesville, Florida 32611, Department of Chemistry, Youngstown State University, Youngstown, Ohio 44555, Instituto de Química, Médica, CSIC, Juan de la Cierva, 3, 28006-Madrid, Spain, and Departmento de Química, C-9, Universidad Autónoma de Madrid, Cantoblanco, 28049-Madrid, Spain

Received: May 9, 2002; In Final Form: July 29, 2002

In our continuing effort to identify NMR spin−spin coupling constants as fingerprints for hydrogen bond type and use these to obtain structural information, EOM-CCSD calculations have been performed to determine one-bond ($^{1d}J_{H-H}$) and three-bond ($^{3d}J_{X-M}$) spin−spin coupling constants across X−H···H−M dihydrogen bonds for complexes with $^{13}C-^{1}H$, $^{15}N-^{1}H$, and $^{17}O-^{1}H$ proton-donor groups and proton-acceptor metal hydrides $^{7}Li-^{1}H$ and $^{23}Na-^{1}H$. Unlike two-bond spin−spin coupling constants across N−H−N, N−H−O, O−H−O, and Cl−H−N hydrogen bonds that are determined solely by the Fermi-contact term, $^{1d}J_{H-H}$ receives nonnegligible contributions from the paramagnetic spin−orbit and diamagnetic spin−orbit terms. However, these terms tend to cancel, so that the curve for the distance dependence of $^{1d}J_{H-H}$ is determined by the distance dependence of the Fermi-contact term. The value of $^{1d}J_{H-H}$ is dependent on the nature of the proton donor and proton acceptor, and the relative orientation of the bonded pair. Hence, it would be difficult to extract structural information from experimentally measured coupling constants unless EOM-CCSD calculations were performed on a model complex that closely resembles the experimental complex. $^{3d}J_{C-Li}$ values for the equilibrium structures of seven linear complexes stabilized by C−H···H−Li bonds are dependent on C−Li distances, and are also sensitive to structural changes which remove any one of these four atoms from the dihydrogen bond. $^{3d}J_{O-M}$ for the complexes HOH:HLi and HOH:HNa exhibit unusual behavior as a function of the O−M distance, increasing with increasing distance through a change of sign, reaching a maximum, and then subsequently decreasing.

Introduction

In the previous paper in this issue,[1] we examined the structural, energetic, bonding, and IR spectroscopic properties of complexes with dihydrogen bonds. In this paper, we will further investigate these complexes, focusing now on NMR spin−spin coupling constants across dihydrogen bonds. This work complements our prior studies directed at identifying fingerprints for hydrogen bond type and obtaining structural information about hydrogen-bonded complexes from NMR coupling constants. In particular, we will investigate one-bond $^{1}H-^{1}H$ spin−spin couplings ($^{1d}J_{H-H}$) and three-bond X−M spin−spin couplings ($^{3d}J_{X-M}$) across X−H···H−M dihydrogen bonds. (We use the designation ^{nd}J to indicate the number of bonds (n) between coupled atoms across a dihydrogen bond (d); this notation is similar to that used for coupling across conventional hydrogen bonds, ^{nh}J.) The complexes investigated have C−H, N−H, and O−H groups as proton donors, and the metal hydrides LiH and NaH as proton acceptors. Crabtree has reported experimental $^{1d}J_{H-H}$ coupling constants involving metal hydrides across intramolecular dihydrogen bonds.[2] However, detailed ab initio investigations of such couplings have not been reported previously. Our emphasis will be on the dependence of one-bond and three-bond spin−spin coupling constants on the nature of the proton-donor group and proton-acceptor metal hydride, the H−H distance, and the orientation of the proton-donor and proton-acceptor species. To the extent possible, we will relate the NMR properties to the properties of these same complexes discussed in the previous paper.[1] The work reported in this paper is a natural extension of our previous ab initio studies of spin−spin coupling constants across conventional X−H···Y hydrogen bonds.[3−17]

Methods

The one-bond H−H and three-bond X−M NMR spin−spin coupling constants across X−H···H−M dihydrogen bonds have been evaluated for the complexes described in the preceding paper that have $^{13}C-^{1}H$, $^{15}N-^{1}H$, and $^{17}O-^{1}H$ as proton donors, and $^{1}H-^{7}Li$ and $^{1}H-^{23}Na$ as proton acceptors. Coupling constants have been computed using the equation-of-motion coupled cluster singles and doubles method (EOM-CCSD) employing the CI-like approximation.[18−21] Because spin−spin coupling constants across dihydrogen bonds have not been previously investigated, we have evaluated all terms that contribute to the total coupling constant. These include the paramagnetic spin−orbit (PSO), diamagnetic spin−orbit (DSO), Fermi-contact (FC), and spin dipole (SD) terms. For these calculations, we have used the qz2p basis set of Ahlrichs et al.[22] on the hydrogen atoms involved in the dihydrogen bond,

† Quantum Theory Project, University of Florida.
‡ Department of Chemistry, Youngstown State University.
§ Instituto de Química, Médica.
|| Departmento de Química, C-9, Universidad Autónoma de Madrid.

10.1021/jp021160v CCC: $22.00
Published on Web 09/14/2002

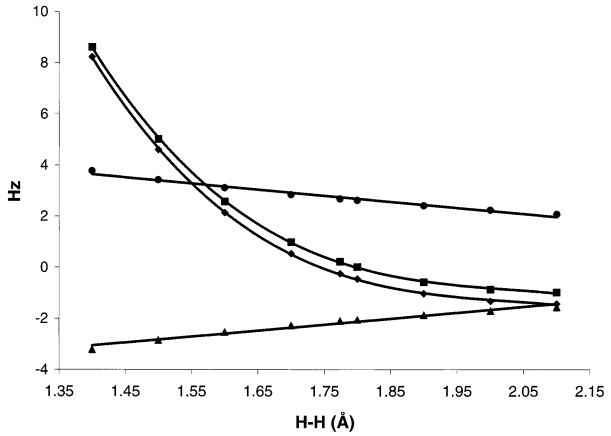

Figure 1. PSO, DSO, and Fermi-contact terms and total $^{1d}J_{H-H}$ as a function of H−H distance for NCH:HLi. ■ = $^{1d}J_{H-H}$; ◆ = FC; ▲ = PSO; ● = DSO.

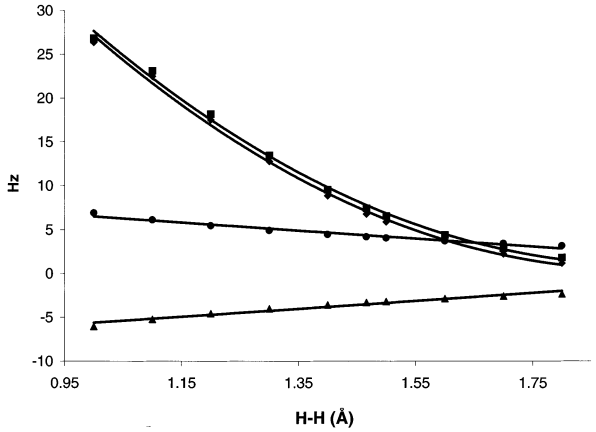

Figure 2. PSO, DSO, and Fermi-contact terms and total $^{1d}J_{H-H}$ as a function of H−H distance for CNH:HLi. Symbol definitions are the same as in Figure 1.

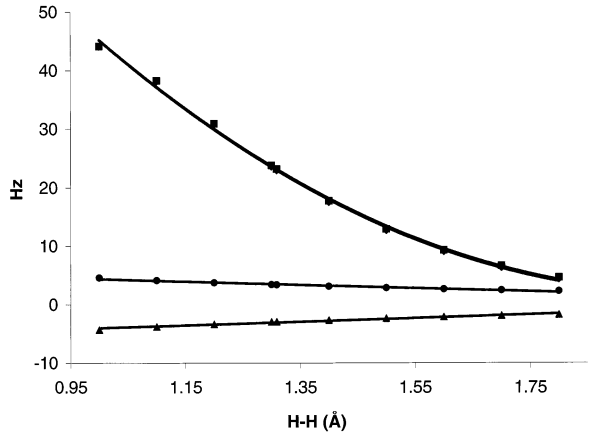

Figure 3. PSO, DSO, and Fermi-contact terms and total $^{1d}J_{H-H}$ as a function of H−H distance for LiNCH$^+$:HLi. Symbol definitions are the same as in Figure 1.

and qzp on nonhydrogen atoms except for Li and Na. This basis set is not available for these atoms, so the corresponding triple-split basis sets were used. Hydrogen atoms not involved in the dihydrogen bond have been described by the Dunning cc-pVDZ basis.[23−25] Coupling constants have been computed for each equilibrium structure, and for the optimized linear structures of CNH:HLi and CNH:HNa. In addition, the dependence of the total coupling constant and the PSO, DSO, FC, and SD terms on the H···H distance and the orientation of the proton donor and proton acceptor have been investigated. Spin−spin coupling constants were computed using the ACES II program.[26] All calculations were carried out on the Cray SV1 computer at the Ohio Supercomputer Center.

Results and Discussion

$^{1d}J_{H-H}$. Total ^{1}H−^{1}H spin−spin coupling constants ($^{1d}J_{H-H}$) obtained from PSO, DSO, FC, and SD components have been computed as a function of the H···H distance for linear $C_{\infty v}$ structures of NCH:HLi, NCH:HNa, CNH:HLi, CNH:HNa, and LiNCH$^+$:HLi, and nonlinear structures of C_1 symmetry derived from the equilibrium structures of HOH:HLi and HOH:HNa. At all distances the SD term is negligible, ranging from −0.04 to −0.20 Hz in complexes with C−H as the proton donor, −0.09 to −0.34 Hz in complexes with N−H as the donor, and −0.11 to +0.16 in complexes with O−H as the donor. Unlike N−N, N−O, O−O, and Cl−N coupling constants across conventional X−H−Y hydrogen bonds which are determined solely by the Fermi-contact term,[4,5,8] H−H couplings have nonnegligible contributions from both the PSO and DSO terms. Total $^{1d}J_{H-H}$ and the PSO, DSO, and FC terms for NCH:HLi are plotted as a function of the H···H distance in Figure 1. Both $^{1d}J_{H-H}$ and the Fermi-contact term vary quadratically with the H···H distance, while the PSO and DSO terms vary linearly. Because PSO and DSO terms have similar magnitudes but opposite signs, these two terms tend to cancel, and the shape of the $^{1d}J_{H-H}$ curve is determined by the shape of the Fermi-contact curve. (The approximate cancellation of PSO and DSO terms observed for these complexes has been observed previously in molecules.[19]) At a given H···H distance, the Fermi-contact term is 0.4 to 0.5 Hz less than $^{1d}J_{H-H}$. However, both $^{1d}J_{H-H}$ and the Fermi-contact term change sign as a function of distance, with the sign change occurring near the equilibrium distance. This suggests that it would be difficult to experimentally measure H−H couplings in such systems because of their small magnitudes. Moreover, even if these could be measured, extracting H···H distances from such measurements would also be difficult. Although not shown, plots of $^{1d}J_{H-H}$ and its components for NCH:HNa exhibit the same general characteristics as evident for NCH:HLi in Figure 1. However, at a given distance, the FC term and $^{1d}J_{H-H}$ are always larger for NCH:HNa. Thus, the magnitude of the H−H coupling shows a dependence on the nature of the metal atom in the metal hydride.

Figures 2 and 3 present plots of $^{1d}J_{H-H}$ and its components as a function of the H···H distance for CNH:HLi and LiNCH$^+$:HLi, respectively. Once again, the PSO and DSO terms tend to cancel, and the shape of the $^{1d}J_{H-H}$ curve is determined by the FC term, which is 0.3 to 0.7 Hz less than $^{1d}J_{H-H}$ for CNH:HLi. It should be noted that at a given distance, $^{1d}J_{H-H}$ for CNH:HLi is greater than $^{1d}J_{H-H}$ for NCH:HLi, demonstrating that the value of the H−H coupling constant also varies with the nature of the proton donor. This effect is significantly larger for LiNCH$^+$:HLi than for NCH:HLi. The increase in$^{1d}J_{H-H}$ is consistent with previous results which indicate that two-bond X−Y coupling constants across conventional X−H−Y hydrogen bonds are also larger in charged complexes.[5,8,13] Once again, plots of $^{1d}J_{H-H}$ and its components for CNH:HNa exhibit the same general features as shown in Figure 2 for CNH:HLi.

Figure 4 presents plots of the PSO, DSO, and FC terms and $^{1d}J_{H-H}$ for HOH:HLi. The plots for HOH:HNa have similar characteristics. To generate these plots, the H···H distance was set to 1.00 Å and incremented in steps of 0.10 Å, keeping H_2O and LiH fixed in their orientation in the equilibrium C_1 complex. For these two complexes, the Fermi-contact term is very large

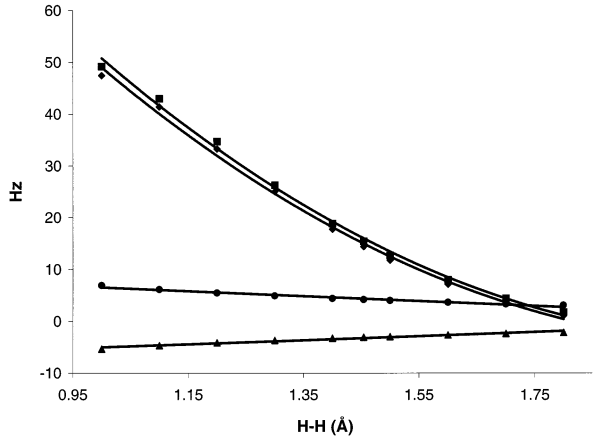

Figure 4. PSO, DSO, and Fermi-contact terms and total $^{1d}J_{H-H}$ as a function of H−H distance for HOH:HLi. Symbol definitions are the same as in Figure 1.

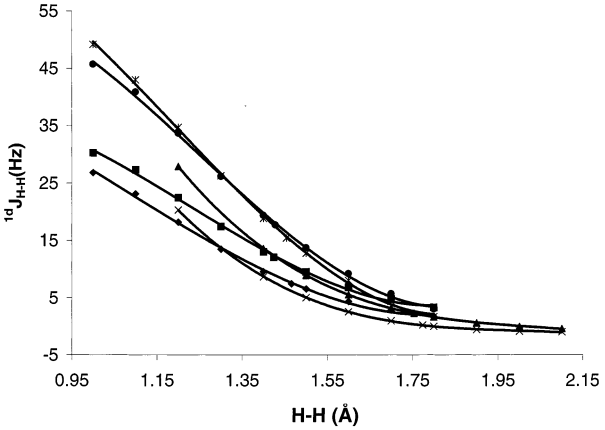

Figure 5. $^{1d}J_{H-H}$ as a function of the H−H distance for complexes stabilized by dihydrogen bonds. * HOH:HLi; ● HOH:HNa; ◆ CNH:HLi; ■ CNH:HNa; × NCH:HLi; ▲ NCH:HNa.

at short H−H distances and near the equilibrium distance. Both the PSO and DSO terms are nonnegligible, but again tend to cancel. As a result, the Fermi-contact term determines the distance dependence of $^{1d}J_{H-H}$.

It is apparent from Figures 1−4 that the DSO and PSO terms are not very sensitive to the nature of the proton donor or proton acceptor. For example, at an H···H distance of 1.40 Å, the PSO contribution to $^{1d}J_{H-H}$ for the entire set of dihydrogen-bonded complexes varies by about 1 Hz, whereas the DSO contribution varies by about 2 Hz. In contrast, the Fermi-contact term and $^{1d}J_{H-H}$ vary by 10 and 11 Hz, respectively. The dependence of $^{1d}J_{H-H}$ on the nature of the proton donor and proton acceptor can be readily seen from Figure 5, which presents plots of $^{1d}J_{H-H}$ versus the H···H distance for the six neutral complexes NCH:HLi, NCH:HNa, CNH:HLi, CNH:HNa, HOH:HLi, and HOH:HNa. At short H···H distances, $^{1d}J_{H-H}$ is largest when H_2O is the proton donor, but the value of $^{1d}J_{H-H}$ decreases most rapidly with increasing H···H distance in these complexes. A comparison of HCN and HNC as donors shows that $^{1d}J_{H-H}$ is larger at shorter distances when NCH is the proton donor, but larger at slightly longer distances when CNH is the donor. At very long distances, the value of $^{1d}J_{H-H}$ shows little dependence on the nature of the donor, because of course, $^{1d}J_{H-H}$ must eventually go to zero. It is also interesting to note that $^{1d}J_{H-H}$ is larger when HNa is the proton acceptor and either HCN or HNC is the donor. However, when H_2O is the donor, $^{1d}J_{H-H}$ is larger at short distances when HLi is the acceptor, but there is a crossover

TABLE 1: Total ^{1}H−^{1}H Spin−Spin Coupling Constants ($^{1d}J_{H-H}$, Hz) and Components of $^{1d}J_{H-H}$ for Optimized Structures of Complexes with Dihydrogen Bonds

complex	R_e(H−H, Å)	PSO	DSO	FC	$^{1d}J_{H-H}$
$LiNCH^+$:HLi	1.309	−2.91	3.34	22.60	22.83
$NaNCH^+$:HLi	1.429	−2.77	3.26	10.74	11.03
NCH:HLi	1.774	−2.10	2.67	−0.25	0.22
NCCCH:HLi	1.809	−2.08	2.63	−0.60	−0.01[a]
ClCCH:HLi	1.930	−1.87	2.45	−0.99	−0.47
FCCH:HLi	1.950	−1.83	2.40	−1.03	−0.52
HCCH:HLi	1.978	−1.76	2.33	−1.07	−0.55
NCH:HNa	1.754	−2.32	2.94	1.79	2.30
CNH:HLi (eq)	1.468	−3.28	4.10	6.73	7.38
linear structure	1.466	−3.32	4.15	6.76	7.43
CNH:HNa (eq)	1.426	−3.57	4.46	11.35	12.06
linear structure	1.424	−3.60	4.49	11.32	12.02
HOH:HLi	1.454	−3.07	4.16	14.37	15.38
HOH:HNa	1.428	−3.67	5.01	16.40	17.65

[a] The SD term was not computed for this complex.

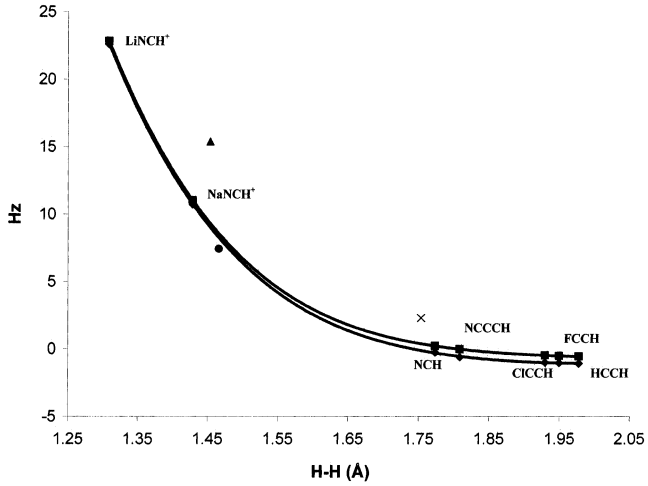

Figure 6. Fermi-contact term and $^{1d}J_{H-H}$ for the equilibrium structures stabilized by C−H···H−Li dihydrogen bonds. The points used to construct the curve are labeled to identify the C−H proton donor. ■ = $^{1d}J_{H-H}$; ◆ = FC; ▲ $^{1d}J_{H-H}$ HOH:HLi; ● $^{1d}J_{H-H}$ CNH:HLi; × $^{1d}J_{H-H}$ NCH:HNa.

point near an H···H distance of 1.30 Å, after which $^{1d}J_{H-H}$ is greater when NaH is the acceptor.

Table 1 presents H−H distances, total H−H spin−spin coupling constants $^{1d}J_{H-H}$, and the PSO, DSO, and FC terms for the equilibrium structures of all complexes investigated in this study. Data for the optimized $C_{\infty v}$ structures of CNH:HLi and CNH:HNa are also included. The first seven complexes have LiH as the proton acceptor and include both cationic and neutral complexes, and are arranged in order of increasing H···H distance. This order is also the order of decreasing $^{1d}J_{H-H}$ and decreasing FC. It should be noted that $^{1d}J_{H-H}$ changes sign in this series. Figure 6 presents a plot of $^{1d}J_{H-H}$ and the Fermi-contact term for the equilibrium structures of these complexes. Note that each data set can be fitted by a single curve, and that the two curves are almost superimposable. This curve is presented as a tool for predicting $^{1d}J_{H-H}$ for complexes with linear C−H···H−Li dihydrogen bonds.

In the preceding paper,[1] we observed that the binding energies of complexes with C−H···H−Li dihydrogen bonds vary quadratically with the H−H distance, and linearly with the amount of electron density at the H···H bond critical point. Because $^{1d}J_{H-H}$ shows a similar distance dependence, $^{1d}J_{H-H}$ also correlates with binding energies and charge densities at the H···H bond critical point. For the complexes with C−H···H−Li dihydrogen bonds, these variables are related by the following

equations

$$^{1d}J_{H-H} = (0.0652BE^2 + 1.11BE + 3.76)\text{Hz, with } n = 7,\ r^2 = 0.981 \quad (1)$$

$$^{1d}J_{H-H} = (12\,188.5\rho_{bcp}{}^2 - 272.3\rho_{bcp} + 0.85)\text{Hz, with } n = 7,\ r^2 = 0.999 \quad (2)$$

where BE is the binding energy in kcal mol^{-1} and ρ_{bcp} the charge density at the H···H bond critical point in e au^{-3}.

The equilibrium distance is that distance at which the binding energy has its maximum value. It is not, however, the distance at which $^{1d}J_{H-H}$ and the electron density at the bond critical point have extremum values, since both $^{1d}J_{H-H}$ and the electron density at the bond critical point increase as the H···H distance decreases. Because in a closely related series of complexes increasing binding energies are accompanied by decreasing equilibrium distances, correlations between binding energies and other distance-related properties should be expected. What is perhaps the most interesting correlation is that between $^{1d}J_{H-H}$ and the electron density at the bond critical point because this relates an NMR property to the electronic features of the dihydrogen bond.

How do the values of $^{1d}J_{H-H}$ for the equilibrium structures of NCH:HNa, CNH:HLi, and HOH:HLi compare with the $^{1d}J_{H-H}$ curve shown for complexes with C−H···H−Li dihydrogen bonds in Figure 6? The value of $^{1d}J_{H-H}$ for NCH:HNa is indicated in Figure 6 by an "x". That the "x" is not closer to the $^{1d}J_{H-H}$ curve is not surprising, given that the equilibrium values of $^{1d}J_{H-H}$ for NCH:HLi and NCH:HNa differ by 2.1 Hz, even though their equilibrium distances differ by only 0.02 Å. This is also consistent with Figure 5, which shows that $^{1d}J_{H-H}$ is greater for NCH:HNa than NCH:HLi over the entire range of distances considered. The solid "circle" in Figure 6 represents the value of $^{1d}J_{H-H}$ for CNH:HLi at its equilibrium distance. This circle lies close to the curve because the curves for NCH:HLi and CNH:HLi cross (Figure 5), and the values of $^{1d}J_{H-H}$ for these two complexes differ by only 1.3 Hz at the CNH:HLi H···H equilibrium distance of 1.466 Å. The solid "triangle" in Figure 6 indicates the value of $^{1d}J_{H-H}$ for HOH:HLi at its equilibrium distance. This value lies far from the curve, so that the distance dependence of $^{1d}J_{H-H}$ for complexes with C−H···H−Li dihydrogen bonds is not useful for predicting $^{1d}J_{H-H}$ for HOH:HLi. This is not surprising, given the very different structures of these complexes.[1]

Our investigation of the geometry dependence of $^{1d}J_{H-H}$ has thus far been limited to its dependence on the H···H distance. We have also investigated the dependence of $^{1d}J_{H-H}$ on changes in the H_b-H_a-C and H_a-H_b-Li angles in the cationic complex $LiNCH_a^+$:H_bLi. This complex was chosen because its equilibrium structure is linear and $^{1d}J_{H-H}$ is large at equilibrium. To investigate the dependence of $^{1d}J_{H-H}$ on the H_b-H_a-C angle, a rotational axis was placed through H_a perpendicular to the H_a-H_b-Li line, and the proton-donor ion was rotated about this axis, keeping the H···H distance and intramolecular distances and angles constant at their equilibrium values. A similar procedure was used to determine the dependence of $^{1d}J_{H-H}$ on the H_a-H_b-Li angle, in which case LiH was rotated about an axis placed through H_b perpendicular to the $C-H_a-H_b$ line. The variations in $^{1d}J_{H-H}$ that occur with these rotations are shown graphically in Figure 7. It is apparent from this figure that the two rotations that destroy the linear C−H···H−Li arrangement have opposite effects. The rotation that removes C from the H_a-H_b-Li line decreases the value of $^{1d}J_{H-H}$,

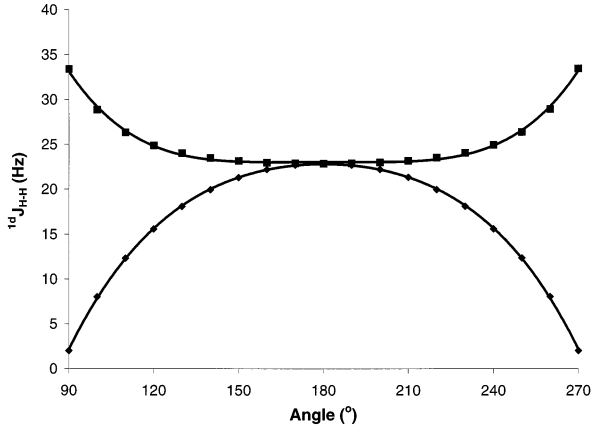

Figure 7. Variation of $^{1d}J_{H-H}$ with changes in $<H_a-H_b-Li$ and $<H_b-H_a-C$, illustrated for $LiNCH_a^+$:H_bLi. ■ $<H_a-H_b-Li$; ◆ $<H_b-H_a-C$.

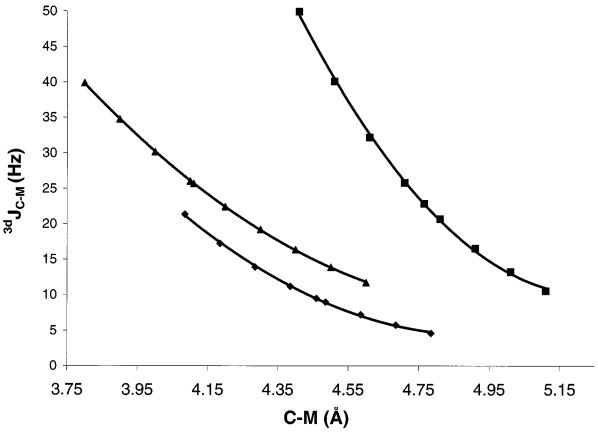

Figure 8. $^{3d}J_{C-M}$ as a function of C−M distance for NCH:HLi, NCH:HNa, and $LiNCH^+$:HLi. ◆ CNH:HLi; ■ CNH:HNa; ▲ $LiNCH^+$:HLi.

whereas the rotation that removes Li from the $C-H_a-H_b$ line increases $^{1d}J_{H-H}$. The curve showing the variation of $^{1d}J_{H-H}$ with the H_a-H_b-Li angle is flatter near the linear structure than the H_b-H_a-C curve, that is, $^{1d}J_{H-H}$ changes more rapidly with changes in the H_b-H_a-C angle. A 30° change in this angle decreases $^{1d}J_{H-H}$ by 1.53 Hz, whereas, a 30° change in the H_a-H_b-Li angle increases $^{1d}J_{H-H}$ by only 0.33 Hz. Changes of 60° in these two angles decrease and increase $^{1d}J_{H-H}$ by 7.26 and 2.07 Hz, respectively. These results suggest that if coupling constants for isolated complexes stabilized by C−H···H−M and N−H···H−M dihydrogen-bonds were measured, these measurements could be used to obtain intermolecular H···H distances provided that the X−H···H−M dihydrogen bond was linear or deviated only slightly from linearity. However, in systems with intramolecular X−H···H−M dihydrogen bonds, the hydrogen-bond geometry is usually nonlinear, so that both distance and angular dependencies of $^{1d}J_{H-H}$ would need to be taken into account, or other coupling constants measured, to extract useful structural information. The situation is also complicated by the fact that the value of $^{1d}J_{H-H}$ is dependent on the nature of the proton-donor X−H group and the nature of the metal.

$^{3d}J_{X-M}$. $^{3d}J_{X-M}$ for complexes NCH:HLi, CNH:HLi, $LiNCH^+$:HLi, NCH:HNa, and CNH:HNa receives negligible contributions from the PSO, DSO, and SD terms, and FC approximates $^{3d}J_{X-M}$ to within 0.1 Hz. In this respect, $^{3d}J_{X-M}$ resembles $^{2h}J_{X-Y}$ across conventional N−H−N, N−H−O, O−H−O, and Cl−H−N hydrogen bonds.[5,8,13] The variation of $^{3d}J_{C-M}$ as a function of distance depends on the nature of M and the charge on the complex. Figure 8 shows the distance dependence of $^{3d}J_{C-M}$

TABLE 2: X−M Distances (R_e, Å) and Three-bond Spin−Spin Coupling Constants ($^{3d}J_{X-M}$, Hz, and $^{3d}K_{X-M}$, N/m^{3}A^2) for Equilibrium Structures of Complexes with Dihydrogen Bonds

complex	R_e(C−M)	FC	$^{3d}J_{C-M}$[a]	$^{3d}K_{C-M}$ ($\times 10^{19}$)
$LiNCH^+$:HLi	4.109	25.65	25.69	21.88
$NaNCH^+$:HLi	4.186	20.49	20.53	17.49
NCH:HLi	4.459	9.51	9.53	8.12
NCCCH:HLi[b]	4.492	9.59	9.60	8.18
ClCCH:HLi	4.605	7.50	7.52	6.41
FCCH:HLi	4.623	7.45	7.46	6.35
HCCH:HLi	4.651	6.22	6.24	5.31
NCH:HNa	4.765	22.84	22.87	28.60
complex	R_e(N−M)	FC	$^{3d}J_{N-M}$[c]	$^{3d}K_{N-M}$ ($\times 10^{19}$)
CNH:HLi (eq)	3.967	−6.99	−7.00	14.79
linear	4.101	−7.33	−7.34	15.51
CNH:HNa (eq)	4.248	−16.82	−16.85	52.29
linear	4.392	−17.63	−17.68	54.87

complex	R_e(O−M)	PSO	DSO	FC	SD	$^{3d}J_{O-M}$	$^{3d}K_{O-M}$ ($\times 10^{19}$)
HOH:HLi	1.896	0.08	−0.02	−0.54	0.03	−0.45	0.71
HOH:HNa	2.277	0.72	−0.01	12.20	0.05	12.96	−30.06

[a] The absolute values of the PSO, DSO, and SD terms do not exceed 0.02 Hz. [b] The SD term was not computed. [c] PSO, DSO, and SD terms vary from 0.00 to −0.03 Hz.

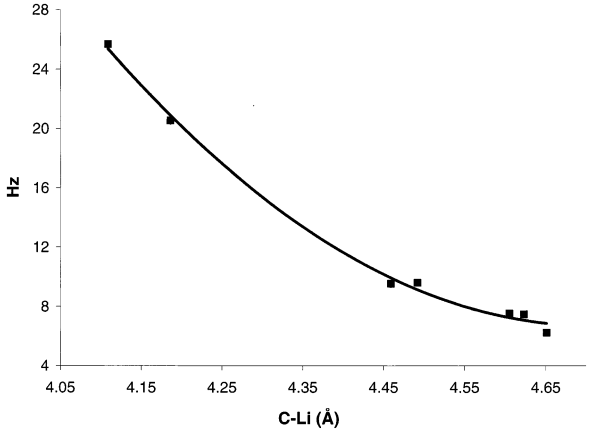

Figure 9. Fermi-contact term and $^{3d}J_{C-Li}$ versus the C−Li distance for complexes stabilized by C−H···H−Li dihydrogen bonds. ■ = $^{3d}J_{C-Li}$; ◆ = FC.

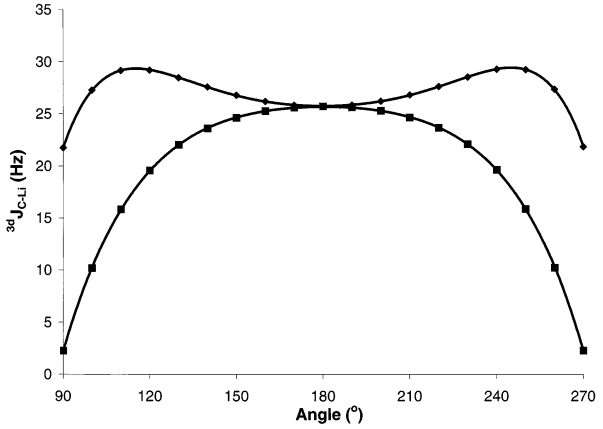

Figure 10. Variation of $^{3d}J_{C-Li}$ with changes in H_a-H_b-Li and H_b-H_a-C angles, illustrated for $LiNCH_a^+$:H_bLi. ■ $<H_a-H_b-Li$; ◆ $<H_b-H_a-C$.

for NCH:HLi, NCH:HNa, and $LiNCH^+$:HLi. Thus, over a range of distances surrounding the equilibrium distances, $^{3d}J_{C-Na}$ is significantly greater than $^{3d}J_{C-Li}$, reflecting the dependence on the metal. Moreover, at a given distance, $^{3d}J_{C-Li}$ for $LiNCH^+$:HLi is also greater than $^{3d}J_{C-Li}$ for neutral NCH:HLi. It should be noted, however, that when comparing coupling constants involving different atoms, it is the reduced coupling constants $^{3d}K_{C-M}$ that should be used. However, general statements made about relationships between $^{3d}J_{X-M}$ for different X and M are valid for $^{3d}K_{X-M}$, although these quantities may differ in sign. Since it is $^{3d}J_{X-M}$ that is measured experimentally, $^{3d}J_{X-M}$ values will be discussed below.

Table 2 presents X−M distances, the Fermi-contact term, $^{3d}J_{X-M}$ and $^{3d}K_{X-M}$ for the equilibrium structures of all complexes investigated in this study, and for the optimized linear structures of CNH:HLi and CNH:HNa. The listing of the first seven complexes that have C−H···H−Li dihydrogen bonds is in order of increasing C−Li distance, and decreasing $^{3d}J_{C-Li}$. The curves showing the distance dependence of the Fermi-contact term and $^{3d}J_{C-Li}$ are superimposable, as seen in Figure 9. The equation of the $^{3d}J_{C-Li}$ curve is

$$^{3d}J_{C-Li} = (52R_e^2 - 491R_e + 1163)\text{Hz with } n = 7,\ r^2 = 0.996 \quad (3)$$

where R_e is the C−Li distance in Å. This curve should be useful for the determination of C−Li distances in complexes that have linear C−H···H−Li dihydrogen bonds.

The variation of $^{3d}J_{C-Li}$ as the C−H···H−Li dihydrogen bond is distorted from linearity has also been investigated, again using $LiCNH^+$:HLi. There are four different rotations which remove one of the four atoms involved in the dihydrogen bond from the linear $C-H_a\cdots H_b-Li$ arrangement. Two rotations remove either C or Li from the dihydrogen-bonding axis, keeping the H···H distance fixed at its equilibrium value, and decreasing the C−Li distance. The first is accomplished by rotating $LiNCH_a^+$ about an axis through H_a and perpendicular to the H_a-H_b-Li line, and is measured by the H_b-H_a-C angle. The second involves rotation of LiH_b about an axis through H_b and perpendicular to the $C-H_a-H_b$ line. This rotation is measured by the H_a-H_b-Li angle. The effects of these two rotations are shown graphically in Figure 10. Small perturbations which cause either C or Li to move slightly off the dihydrogen bonding axis produce only small changes in $^{3d}J_{C-Li}$, but these occur in opposite directions. A 30° rotation that removes C from the axis increases $^{3d}J_{C-Li}$ by 1.09 Hz, whereas a 30° rotation that removes Li decreases $^{3d}J_{C-Li}$ by the same amount. The curve for $^{3d}J_{C-Li}$ exhibits a maximum value when the H_b-H_a-C angle

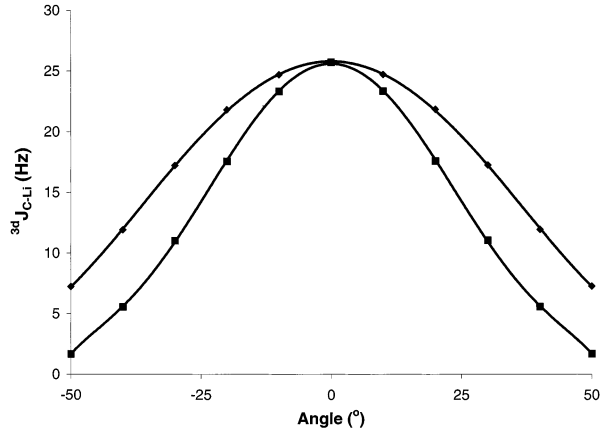

Figure 11. Variation of $^{3d}J_{C-Li}$ with changes in H_a-C-Li and H_b-Li-C angles, illustrated for $LiNCH_a^+$:H_bLi. ■ $<H_b-Li-$ C; ◆ $<H_a-C-Li$.

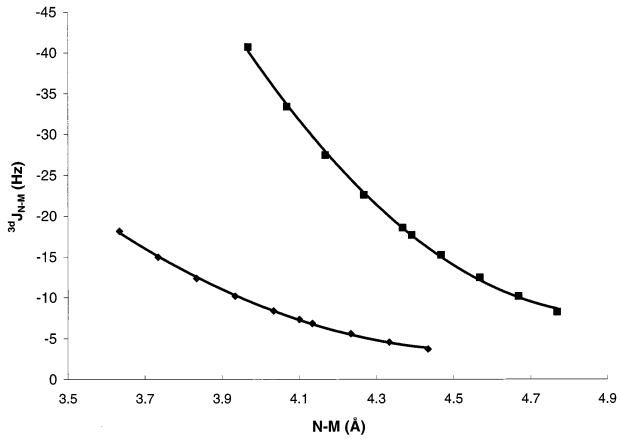

Figure 12. $^{3d}J_{N-M}$ as a function of N−M distance for CNH:HLi and CNH:HNa. ■ CNH:HNa; ◆ CNH:HLi.

is about 115° (245°), and then decreases rapidly. $^{3d}J_{C-Li}$ also decreases rapidly with increasing H_a-H_b-Li angle.

The linearity of the dihydrogen bond may also be destroyed by removing one of the two hydrogens from this bond while keeping the remaining H, C, and Li atoms collinear, and the C−Li distance fixed at its equilibrium value. This may be accomplished either by a rotation of $LiNCH^+$ about an axis through C and perpendicular to the $C-H_b-Li$ line, with the rotation measured by the H_a-C-Li angle, or by a rotation of LiH about an axis through Li and perpendicular to the $Li-H_a-C$ line, measured by the H_b-Li-C angle. Changes in $^{3d}J_{C-Li}$ as a function of these two angles are shown graphically in Figure 11. Removing either one of the hydrogens from the dihydrogen-bonding axis leads to a rapid decrease of $^{3d}J_{C-Li}$, despite the fact that the C−Li distance is unchanged. A 30° change in the H_a-C-Li and H_b-Li-C angles decreases $^{3d}J_{C-Li}$ by 8.49 and 14.67 Hz, respectively. Thus, three-bond couplings across a dihydrogen bond are most effective when the X−H···H−M arrangement is linear. A similar observation was made in a previous study of three-bond N−P couplings across conventional N−H···O−P hydrogen bonds, which are also very sensitive to a linear arrangement of N, H, O, and P atoms.[15,27]

The distance dependence of three-bond $^{15}N-^{7}Li$ and $^{15}N-^{23}Na$ spin−spin coupling constants ($^{3d}J_{N-Li}$ and $^{3d}J_{N-Na}$) for CNH:HLi and CNH:HNa are shown in Figure 12. As is the case for $^{3d}J_{C-Li}$ and $^{3d}J_{C-Na}$, PSO, DSO, and SD terms are negligible, and the Fermi-contact term approximates $^{3d}J_{N-M}$ to within 0.1 Hz. The Fermi-contact term and therefore total $^{3d}J_{N-M}$

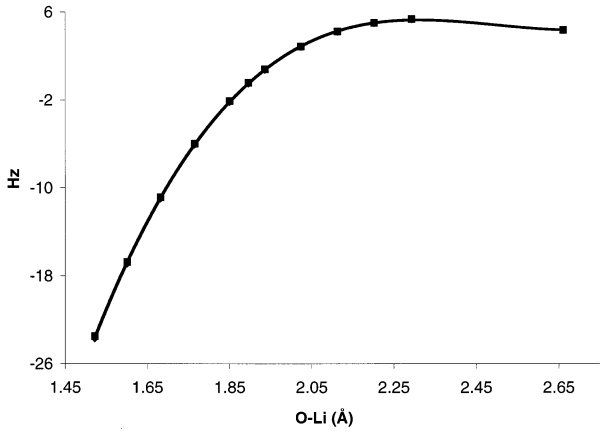

Figure 13. $^{3d}J_{O-Li}$ and the Fermi-contact term as a function of O−Li distance in HOH:HLi. ■ = $^{3d}J_{O-Li}$; ◆ = FC.

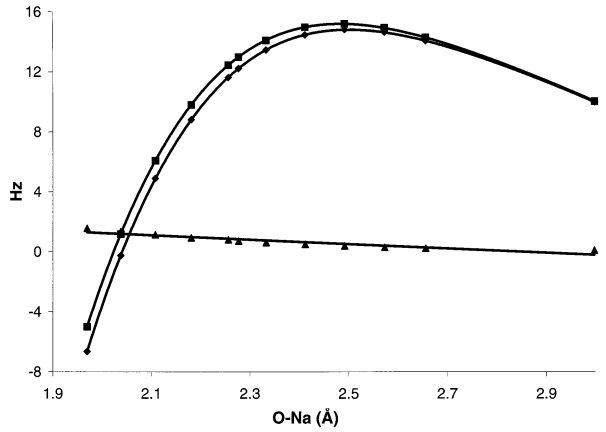

Figure 14. $^{3d}J_{O-Na}$, the Fermi-contact and PSO terms as a function of O−Na distance in HOH:HNa. ■ = $^{3d}J_{O-Na}$; ◆ = FC; ▲ = PSO.

have negative signs. The absolute values of these coupling constants decrease with increasing distance. Consistent with the relationship between $^{3d}J_{C-Li}$ and $^{3d}J_{C-Na}$, the absolute value of $^{3d}J_{N-Na}$ is always greater than $^{3d}J_{N-Li}$ at distances surrounding the equilibrium distances.

Figure 13 presents the distance dependence of the three-bond $^{17}O-^{7}Li$ Fermi-contact term and the total spin−spin coupling constant $^{3d}J_{O-Li}$ across the dihydrogen bond in HOH:HLi. In HOH:HLi the PSO, DSO, and SD terms are negligible. As evident from Figure 13, $^{3d}J_{O-Li}$ is negative at short O−Li distances, changes sign at a distance near the equilibrium distance, and continues to increase with increasing O−Li distance. At an O−Li distance of approximately 2.3 Å, $^{3d}J_{O-Li}$ has its maximum value and then begins to decrease as the O−Li distance increases. This behavior of $^{3d}J_{O-Li}$ is unique with respect to the distance dependence of one- and three-bond couplings across dihydrogen bonds observed in this study. It is also unique in the sense that two-, three-, and four-bond coupling constants across conventional hydrogen bonds always decrease (in an absolute sense) with increasing hydrogen bond distance. Although we do not have a rigorous explanation for this behavior, it must certainly be related to the fact that this coupling does not occur through the dihydrogen bond. The equilibrium structure of this complex has very nonlinear $O-H_a-H_b$ and H_a-H_b-Li arrangements, and a relatively short O−Li distance which allows for direct interaction between these two atoms.

The distance dependence of the PSO and Fermi-contact terms and $^{3d}J_{O-Na}$ for HOH:HNa are presented graphically in Figure 14. The DSO and SD terms are negligible, but at short O−Na distances, the PSO term is significant, with the result that the

FC and $^{3d}J_{O-Na}$ curves are not superimposable. As the O−Na distance increases, the PSO term becomes less important, and the FC and $^{3d}J_{O-Na}$ curves approach each other. Once again, $^{3d}J_{O-Na}$ is negative at short distances, changes sign, and continues to increase as the O−Na distance increases. At a distance of about 2.5 Å, $^{3d}J_{O-Na}$ has its maximum value and then decreases as the O−Na distance increases. Thus, both $^{3d}J_{O-Li}$ and $^{3d}J_{O-Na}$ exhibit the same type of distance dependence. Unfortunately, NMR spin−spin coupling constants involving O atoms are not accessible experimentally because of the large quadrupole moment of the oxygen nucleus. Experimental verification of this intriguing behavior would be most satisfying.

Conclusions

The EOM-CCSD results reported in this study of dihydrogen-bonded complexes support the following statements.

1. $^{1d}J_{H-H}$ for dihydrogen-bonded complexes with C−H, N−H, and O−H as proton-donating groups and LiH and NaH as proton acceptors have nonnegligible contributions from both PSO and DSO terms. Because these terms have similar magnitudes but opposite signs, the shape of the $^{1d}J_{H-H}$ curve as a function of the H···H distance is determined by the Fermi-contact curve.

2. A single $^{1d}J_{H-H}$ curve can be constructed as a function of the H···H distance for the equilibrium structures of complexes with C−H···H−Li dihydrogen bonds. Because binding energies and charge densities at H···H bond critical points for these complexes are also distance-dependent, these properties also correlate with $^{1d}J_{H-H}$.

3. The value of $^{1d}J_{H-H}$ depends on the nature of the proton-donor group and the proton-acceptor metal hydride, the intermolecular H···H distance, and the relative orientation of the dihydrogen-bonded pair. Hence, it would be difficult to extract structural information from experimentally measured coupling constants without assistance from reliable theoretical calculations carried out on complexes specifically modeled for that system.

4. The variation of $^{3d}J_{C-Li}$ as a function of the C−Li distance for the linear equilibrium structures of seven complexes with C−H···H−Li dihydrogen bonds can be fitted by a single curve. However, the value of $^{3d}J_{C-Li}$ is sensitive to structural changes which destroy linearity by removing any one of these four atoms from the dihydrogen bond.

5. Three-bond $^{3d}J_{O-Li}$ and $^{3d}J_{O-Na}$ coupling constants exhibit unusual behavior as a function of the O−Li or O−Na distance, increasing with increasing O−Li or O−Na distance through a change of sign, reaching a maximum, and then subsequently decreasing with increasing distance.

Acknowledgment. This work was supported by the National Science Foundation through grant CHE-9873815 (J.E.D.B.), the Air Force Office of Scientific Research AFOSR F49620-98-0116 (R.J.B.), and the Spanish DGI (Project Nos. BQU-2000-0906 and BQU-2000-0245). The support of these agencies and the continuing support of the Ohio Supercomputer Center are gratefully acknowledged. J.E.D.B. thanks the BBVA Foundation for a Visiting Fellowship at the Universidad Autónoma de Madrid.

References and Notes

(1) Alkorta, I.; Elguero, J.; Mó, O.; Yáñez, M.; Del Bene, J. E. *J. Phys. Chem. A* **2002**, *106*, 9325.
(2) Peris, E.; Lee, J. C.; Rambo, J. R.; Eisenstein, O.; Crabtree, R. H. *J. Am. Chem. Soc.* **1995**, *117*, 3485. Crabtree, R. H. *J. Organomet. Chem.* **1998**, *577*, 111.
(3) Perera, S. A.; Bartlett, R. J. *J. Am. Chem. Soc.* **2000**, *122*, 1231.
(4) Del Bene, J. E.; Perera, S. A.; Bartlett, R. J. *J. Am. Chem. Soc.* **2000**, *122*, 3560.
(5) Del Bene, J. E.; Jordan, M. J. T. *J. Am. Chem. Soc.* **2000**, *122*, 4794.
(6) Del Bene, J. E.; Perera, S. A.; Bartlett, R. J.; Alkorta, I.; Elguero, J. *J. Phys. Chem. A* **2000**, *104*, 7165.
(7) Laynez, J.; Menéndez, M.; Velasco, J. L. S.; Llamas-Saiz, A. L.; Foces-Foces, C.; Elguero, J.; Molina, P.; Alajarín, M. *J. Chem. Soc., Perkins Trans. 2* **1993**, 709.
(8) Del Bene, J. E.; Perera, S. A.; Bartlett, R. J. *J. Phys. Chem. A* **2001**, *105*, 930.
(9) Jordan, M. J. T.; Toh, J. S.-S.; Del Bene, J. E. *Chem. Phys. Lett.* **2001**, *346*, 288.
(10) Del Bene, J. E.; Jordan, M. J. T.; Perera, S. A.; Bartlett, R. J. *J. Phys. Chem. A* **2001**, *105*, 8399.
(11) Del Bene, J. E.; Bartlett, R. J. *J. Am. Chem. Soc.* **2000**, *122*, 10 480.
(12) Chapman, K.; Crittenden, D.; Bevitt, J.; Jordan, M. J. T.; Del Bene, J. E. *J. Phys. Chem. A* **2001**, *105*, 5442.
(13) Del Bene, J. E.; Perera, S. A.; Bartlett, R. J. *Magn. Res. Chem.* **2001**, *39*, S109.
(14) Del Bene, J. E.; Jordan, M. J. T. *J. Mol. Struct. (THEOCHEM)* **2001**, *573*, 11.
(15) Del Bene, J. E.; Perera, S. A.; Bartlett, R. J.; Elguero, J.; Alkorta, I.; Lopez-Leonardo, C.; Alajarin, J. *J. Am. Chem. Soc.* **2002**, *124*, 6393.
(16) Perera, S. A.; Bartlett, R. J. *Magn. Reson. Chem.* **2001**, *39*, S183.
(17) Bartlett, R. J.; Del Bene, J. E.; Perera, S. A. *Structures and Mechanisms: From Ashes to Enzymes*; Eaton, G. R.; Wiley, D. C.; Jardetzky, O., Eds.; ACS Symposium Series, Vol. 827; Oxford University Press: 2002 (in press).
(18) Perera, S. A.; Sekino, H.; Bartlett, R. J. *J. Chem. Phys.* **1994**, *101*, 2186.
(19) Perera, S. A.; Nooijen, M.; Bartlett, R. J. *J. Chem. Phys.* **1996**, *104*, 3290.
(20) Perera, S. A.; Bartlett, R. J. *J. Am. Chem. Soc.* **1995**, *117*, 8476.
(21) Perera, S. A.; Bartlett, R. J. *J. Am. Chem. Soc.* **1996**, *118*, 7849.
(22) Schäfer, A.; Horn, H.; Ahlrichs, R. *J. Chem. Phys.* **1992**, *97*, 2571.
(23) Dunning, T. H., Jr. *J. Chem. Phys.* **1989**, *90*, 1007.
(24) Kendall, R. A.; Dunning, T. H., Jr.; Harrison, R. J. *J. Chem. Phys.* **1992**, *96*, 1358.
(25) Woon, D. E.; Dunning, T. H., Jr. *J. Chem. Phys.* **1993**, *98*, 1358.
(26) ACES II is a program product of the Quantum Theory Project, University of Florida. Authors: Stanton, J. F.; Gauss, J.; Watts, J. D.; Nooijen, M.; Oliphant, N.; Perera, S. A.; Szalay, P. G.; Lauderdale, W. J.; Gwaltney, S. R.; Beck, S.; Balkova, A.; Bernholdt, D. E.; Baeck, K.-K.; Tozyczko, P.; Sekino, H.; Huber, C.; Bartlett, R. J. Integral packages included are VMOL (Almlof, J.; Taylor, P. R.); VPROPS (Taylor, P. R.); ABACUS (Helgaker, T.; Jensen, H. J. Aa.; Jorgensen, P.; Olsen, J.; Taylor, P. R.). Brillouin-Wigner perturbation theory was implement by Pittner, J.
(27) Mishima, M.; Hatanaka, M.; Yokoyama, S.; Ikegami, T.; Wälchli, M.; Ito, Y.; Shirakawa, M. *J. Am. Chem. Soc.* **2000**, *122*, 5883.